Proceedings of the 39th Chinese Control Conference
July 27-29, 2020, Shenyang, China

Design and Implement of Shape Detection for the Soft Manipulator

Shuangquan Zou[1], Yueyong Lv [1], Yuanchen Man[2], Weidi Han[1]

1. School of Astronautics, Harbin Institute of Technology, Harbin 150001, China
E-mail: 18s104179@stu.hit.edu.cn

2. Beijing Aerospace Measurement and Control Technology Co. Ltd, Beijing 100041, China
E-mail: manyuanchen@163.com

Abstract: This paper designs and implements an innovative shape detection system for the soft manipulator to attain the shape reconstruction in real time, which completes the closed-loop control system to enhance control accuracy. Cable encoders are selected as the sensor to measure the length variables for the input of the kinematics model. The kinematics model for unit section is proposed under the assumption of piecewise constant curvature theory, converting the length variables to the curve parameters. Then the unit-section model is extended to the multi-section model based on the novel D-H method, which obtains the posture of the whole manipulator. In addition, the singularity problem can be well disposed employing multivariate Taylor expansion to improve the kinematics model. Finally, we verify respectively the reasonability of the shape detection system from theory and experiment, and the experiment results agree well with the simulation results by MATLAB in real time.

Key Words: soft manipulator, kinematics model, piecewise constant curvature, D-H method

1 Introduction

With the increasing development of computer science, sensor technology and control theory, robotic technology has made rapid progress in the past decade, and the concept of the manipulator is no longer limited to the traditional rigid-link manipulator.

An innovative robot named continuum soft manipulator is emerging, which has triggered considerable attention of a great many researchers [1,3,4,6,8,9]. In comparison to the traditional rigid-link manipulator, the soft manipulator features a continuous backbone with no joints [2,7,10,13], inspired by a physiological structure in nature called muscular hydrostatic skeleton, such as octopus arms, squid tentacles and elephant trunks [5-8]. In spite of the absence of the bone support, it is still able to perform all kinds of flexible actions and complicated shapes to deal with emergencies and changing circumstances, which motivated a recent surge of investigation in prototypes of the soft manipulator. Whereupon plenty of prototypes with high flexibility and compliant grasp have been generated [7,11,14,16] as a feasible solution to many applications in navigation, surgery, and rescue. It makes up the deficiency of rigid-link manipulator in restricted application.

It is because the soft manipulator has the high flexibility and adaptability that the rigid-link manipulator cannot match that makes it extremely difficult to model. What is the most challenging work is to establish an accurate kinematic model for the soft manipulator on account of the infinite degrees of freedom. Moreover, the control and positioning precision of soft manipulator are not satisfactory in the absence of accurate kinematics models. There are some fruitful achievements to be used in the field of kinematics modeling method for soft manipulator [10-13]. I. Walker et al [9] proposed the piecewise constant curvature theory to make a clear definition for kinematics, which put forward the unified coordinate system and formulate the curve parameters. I. Godage et al. [5] presented polynomial form and power exponential form shape functions to improve the kinematics model. From the perspective of experimental analysis, M. Grissom et al. [13] established a set of motion theories that can ensure the safety of 2-DOF continuous robots.

To circumvent these issues, the shape detection system is imperative to feedback shape information to the controller for higher accuracy as the feedback link of the control system. There is a great variety of sensors to select as the element in existing studies [15-18]. Z. Gong [18] adopted the end camera, which can only feedback local information, as shown in Fig.1a). To calculate the shape of the whole soft manipulator, it is necessary to make additional assumptions or optimization methods, which not only reduces the accuracy, but also increases the extra time cost. This is extremely detrimental to real-time control. The inertial sensor used by W. Chao [17] cannot realize continuous distribution so that it is necessary to fuse with the data of each sensor and fit the shape, which leads to poor measurement accuracy, given in Fig.1b).

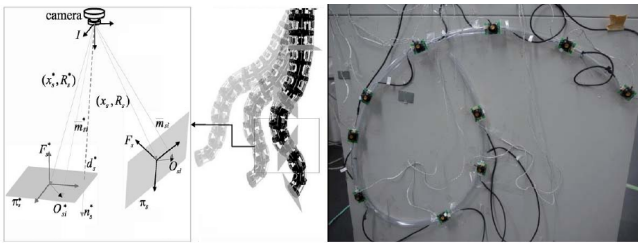

a) The end camera sensor b) The inertial sensor

Fig.1 The shape detection system with different sensors

The arrangement of this paper is as follows: Section 2 describes the composition and operation process of the whole control system we designed, especially the prototype and the distribution of the sensor network in more detail. Then in section 3 the kinematics model for unit-section is built with the help of curve parameters, and it is extended to the multi-section model by the novel D-H method. The multivariate Taylor expansion is employed to supplement the kinematics model in the case of the singularity problem.

*This work is Funded by Science and Technology on Space Intelligent Control Laboratory, No.HTKJ2019KL502014, National Natural Science Foundation of China under Grant 61673135 and 61973100.

Authorized licensed use limited to: IEEE Customer. Downloaded on December 27,2020 at 02:07:31 UTC from IEEE Xplore. Restrictions apply.

In section 4, several simulations are solved out to explain the reasonability of the kinematics model by inputting multiple groups of length variables. In order to further verify the effectiveness of the shape detection system, the experiments are performed to compare with the simulation results.

2 System Description

In this section, a closed-loop control system we designed is elaborated to ensure real-time 3D shape detection and high precision control function, as show in Fig.2

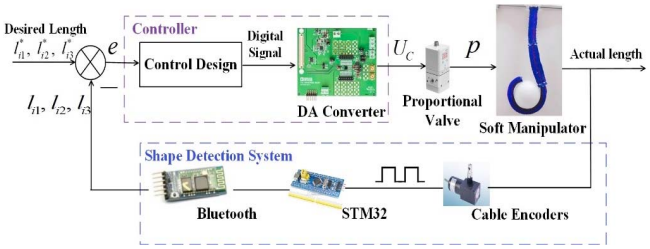

Fig.2 Control System architecture of the soft manipulator

During the control process, the length variables measured by shape detection system are compared with the desired length to produce the error signal e. Then the error signal e is transformed into the control signal U_C by the controller to control the pressure of the proportional valve, so as to control the 3D shape of the soft manipulator, until the top of the soft manipulator gets to the desired position.

2.1 Prototype Manipulator

In the entire control system, the soft manipulator, high flexibility, attaches great importance to realize constant curvature bending as the controlled object.

The pneumatic muscle actuators (PMAs) are identified as the basic unit of the soft manipulator, which is composed of rubber tube and nylon covered on its surface. The prototype applied in our work (see Fig. 3) is constructed by stacking three continuum sections, configured with three or six PMAs for each section. These PMAs can be actuated to extend or contract by filling with different pressure, which are distributed symmetrically in the continuum section. By this means the soft manipulator can be deformed independently in various direction actuated by adjustable pressure.

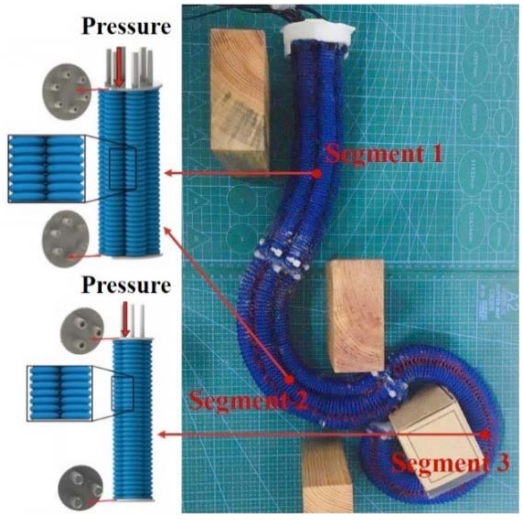

Fig. 3: The structure of the prototype in more details

2.2 Sensor System

A sensor system plays a significant role in the control accuracy to implement the shape detection for the soft manipulator in real-time, equipped with three cable encoders per section as the sensor.

For clarity, the 3D illustration of the sensor system for one section is displayed in Fig.4. Three cable encoders are mounted on the base plate at a radius r_i from the center and $120°$ apart. For the sake of the ideal shape detection effect, the cables are attached tightly on the surface of PMAs, parallel to the continuum section, and change with the length of the PMAs in real-time.

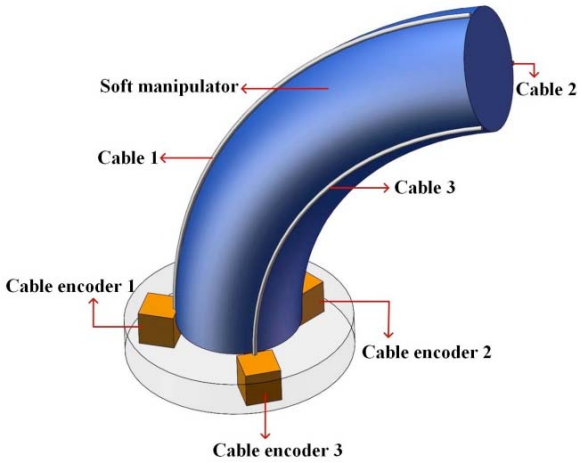

Fig. 4: The 3D illustration of the sensor system for one section

3 Kinematics Model

The kinematics model describes the variation rule of the object position with time from the perspective of the geometry, which is the key to high-precision 3D shape detection and motion control.

In this section, we introduce the kinematics model for the unit section with the help of curve parameters $\{L_i, \phi_i, r_i\}$ in detail. Afterwards, the kinematics model for the unit section is extended to the multi-section by the novel D-H method. Finally, it points out the limitation of the kinematics model we presented and the corresponding solutions.

3.1 Unit-section Model

As we all known, there is a unique line between any two points. Therefore, the conventional rigid manipulator can be defined simply and accurately by the joint angles and link lengths. However, for a soft manipulator, the deformable trunk is displayed with various spatial postures because of the infinite degrees of freedom ideally, resulting in difficulties in establishing accurate kinematics models.

Under the assumption of simplifying the spatial structure for the soft manipulator, the piecewise constant curvature theory is often considered as the effective approach to generating its kinematics model. The main idea of the theory is the curvature of each section is a constant, hence the shape of the unit manipulator both position and direction is described as the positive arc. We proceed in this fashion due to the fact that the prototype presented in this work can achieve bend smoothly in space through specific manufacturing techniques to match with the theoretical kinematics model with less error.

Without loss of generality, the model schematic of the unit

Authorized licensed use limited to: IEEE Customer. Downloaded on December 27,2020 at 02:07:31 UTC from IEEE Xplore. Restrictions apply.

section configured with three cable encoders is illustrated in Fig.5.

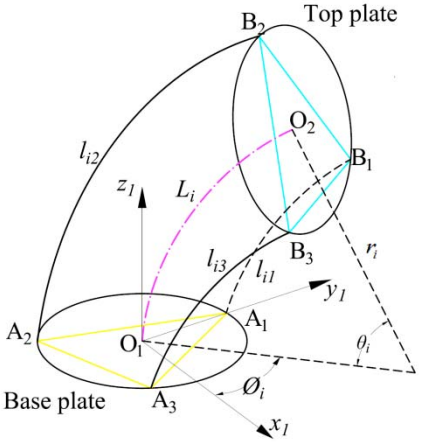

Fig. 5: The model schematic for section 1

Take the center of the base plate as the origin O_1, and the global coordinates $\{O_1 - x_1 y_1 z_1\}$ is established. The neutral line O_1O_2 runs through the center of the section of the backbone, representing the spatial shape of the entire manipulator based on curve parameters $\{L_i, \phi_i, r_i\}$. Note that $r_i \in (0, +\infty)$ is the radius of the neutral line, L_i is the arc length, and ϕ_i is specified as the angle of bending plane relative to the $+X_i$-axis. When the soft manipulator bends, the curve parameters $\{L_i, \phi_i, r_i\}$ vary accordingly in real time. Through the derivation of spatial geometry, the curvature parameters $\{L_i, \phi_i, r_i\}$ are given as follows.

$$L_i(l_{ij}) = (l_{i1} + l_{i2} + l_{i3})/3 \quad (1)$$

$$\phi_i(l_{ij}) = \tan^{-1}\left(\frac{\sqrt{3}(l_{i2} + l_{i3} - 2l_{i1})}{3(l_{i2} - l_{i3})}\right) \quad (2)$$

$$r_i(l_{ij}) = \frac{d(l_{i1} + l_{i2} + l_{i3})}{2\sqrt{l_{i1}^2 + l_{i2}^2 + l_{i3}^2 - l_{i1}l_{i2} - l_{i1}l_{i3} - l_{i2}l_{i3}}} \quad (3)$$

Where $l_{ij} \in \left[(l_{ij})_{\min}, (l_{ij})_{\max}\right]$ is denoted as the lengths of the actuator j for the section i obtained via three cable encoders, i means the section number, and j means the actuator number. $(l_{ij})_{\min}$ and $(l_{ij})_{\max}$ represent the minimum and maximum values respectively that the actuators can stretch. d is determined as the distance between the O_i and actuators. Some known parameters in equations (1)-(3) are indicated in the table 1 specifically.

Table 1: Some essential parameters of the prototype in our work

Parameter	Value
i	{1,2,3}
j	{1,2,3}
d	1cm
$(l_{ij})_{\min}$	12cm
$(l_{ij})_{\max}$	25cm

Combining the arc length formula $L_i = r_i\theta_i$ we're familiar with, the arc angle θ_i and the position vector p_{i+1}^i of the O_{i+1} with respect to the local coordinates $\{O_i - x_i y_i z_i\}$ are demonstrated separately as

$$\theta_i = \frac{2}{3d}\sqrt{l_{i1}^2 + l_{i2}^2 + l_{i3}^2 - l_{i1}l_{i2} - l_{i1}l_{i3} - l_{i2}l_{i3}}, \quad (4)$$

$$p_{i+1}^i = \left[r_i\cos\phi_i(1-\cos\theta_i) \;\; r_i\sin\phi_i(1-\cos\theta_i) \;\; r_i\sin\theta\right]. \quad (5)$$

Apparently, all the above curve parameters are calculated only using the length variables l_{ij}. In other words, we only require the length variables l_{ij} using cable encoders, so as to set up the kinematics model for the unit-section completely.

3.2 Multi-section Model

Unit-section manipulator is an essential model and simple to control, but it cannot satisfy the task demand. As a result, majority of practical application cases involve multi-section manipulator.

The following section introduces the novel D-H method to develop the kinematics model for the multi-section, as shown in Fig.6. Analogous to traditional D-H method for the rigid manipulator, the novel D-H method formulates the coordinate transformation of the adjacent section by the homogeneous transformation matrix (HTM) as well. What is different is the HTM is expressed by curve parameters $\{L_i, \phi_i, r_i\}$ when considering the structural characteristics of the soft manipulator. The HTM is derived as follows, consisting of the rotation and translation of the coordinate system.

$$T_i = \begin{bmatrix} R_{i+1}^i & p_{i+1}^i \\ 0 & 1 \end{bmatrix}_{4\times4} \quad (6)$$

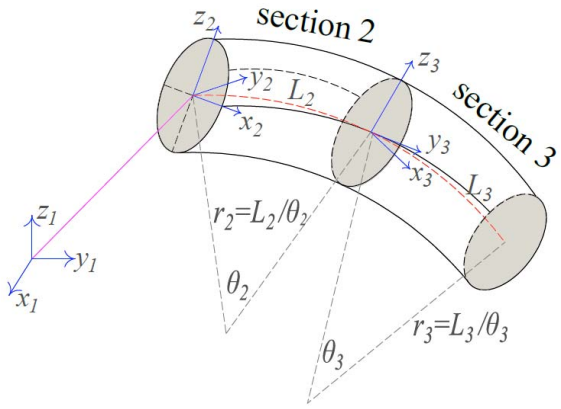

Fig. 6: The model schematic for N sections (N=3)

Where p_{i+1}^i is the translation vector we got before, and R_{i+1}^i is selected as the rotation matrix, which is the only unknown element in the HTM. Thus, the solution procedure of the rotation matrix R_{i+1}^i is yielded as follows.

Authorized licensed use limited to: IEEE Customer. Downloaded on December 27,2020 at 02:07:31 UTC from IEEE Xplore. Restrictions apply.

$$R_{i+1}^{i} = Rot(z_i,\phi_i)Rot(y_i,\theta_i/2)Trans(z_i,\|O_iO_{i+1}\|)$$
$$Rot(y_i,\theta_i/2)Rot(z_i,-\phi_i)$$
$$= \begin{bmatrix} \cos^2\phi_i(\cos\theta_i-1)+1 & \sin\phi_i\cos\phi_i(\cos\theta_i-1) \\ \sin\phi_i\cos\phi_i(\cos\theta_i-1) & \sin^2\phi_i(\cos\theta_i-1)+1 \\ -\cos\phi_i\sin\theta_i & -\sin\phi_i\sin\theta_i \end{bmatrix}$$
$$\begin{bmatrix} \cos\phi_i\sin\theta_i \\ \sin\phi_i\sin\theta_i \\ \cos\theta_i \end{bmatrix} \quad (7)$$

According to multiplying the rotation matrix in sequence for each step, the transformation from coordinates $\{O_i - x_i y_i z_i\}$ to coordinates $\{O_{i+1} - x_{i+1} y_{i+1} z_{i+1}\}$ is figured out. Similarly, the rotation matrix R_N^1 for the neutral line of the whole manipulator relative to the global coordinates $\{O_1 - x_1 y_1 z_1\}$ is equivalent to

$$R_N^1 = \prod_{i=2}^{N} R_i^{i-1}. \quad (8)$$

Furthermore, the position vector P_i of the O_{i+1} with respect to the global coordinates $\{O_1 - x_1 y_1 z_1\}$ is satisfied as

$$P_i = \begin{cases} p_{i+1}^{i}, & i=1 \\ P_{i-1} + R_i^1 p_i^{i-1}, & i>1 \end{cases} \quad (9)$$

In conclusion, the set of the position vector $\{P_1, P_2, P_3\}$ is solved iteratively to establish the kinematics model of the multi-section soft manipulator based on the novel D-H method.

3.3 Limitation of the Kinematics Model

There is an obvious limitation in the kinematics model we presented above, which is a numerical issue substantially. In particular, when all the actuators have the same length, namely $l_{i1} = l_{i2} = l_{i3}$, the denominator of the formula (3) is equal to 0, rendering the radius of curvature infinity. What an unreliable result to describe the arc. Likewise, the numerator and denominator of formula (2) are 0 simultaneously to make the bending plane angle undefined, which is a singularity problem.

In summary, the space shape of the soft manipulator is cylindrical under the condition of $l_{i1} = l_{i2} = l_{i3}$, so the kinematics model based on curve parameters is no longer applicable. To circumvent the limitation, the multivariate Taylor expansion of formula (2) at 0 is employed to eliminate the singularity. The most suitable Taylor expansion order is chosen 11, referring [7]. For instance, the result of Taylor expansion for $\left[p_{i+1}^{i}\right]_1$ is showed below as

$$\left[p_{i+1}^{i}\right]_1 = -\frac{A_2A_4A_1^4}{837019575d^9} + \frac{A_2A_4A_1^3}{4133430d^7} - \frac{A_2A_4A_1^2}{32805d^5} + \frac{A_2A_4A_1}{486d^3} - \frac{A_2A_4}{18d} \quad (9)$$

Where $A_1 = l_{i1}^2 + l_{i2}^2 + l_{i3}^2 - l_{i1}l_{i2} - l_{i1}l_{i3} - l_{i2}l_{i3}$, $A_2 = 2l_{i1} - l_{i2} - l_{i3}$, $A_4 = l_{i1} + l_{i2} + l_{i3}$. The test of the singularity solution will be mentioned in section 4.1.

4 Simulation and Experiment Validation

Here, several simulations are carried out by MATLAB to verify theoretically the correctness of the kinematics model we proposed, and then experiments are conducted to examine prototype behavior and the effectiveness of the shape detection system, compared against the simulation results of kinematics model in real-time.

4.1 Simulation results

The 3D shape of the multi-section soft manipulator is simulated in all kinds of situations to accomplish theoretical verification by artificially inputting multiple groups of length variables.

Firstly, without loss of generality, we input 9 different length variables (see table 2) to obtain the curved spatial shapes for each section, as seen in Fig.7. Different colors represent different sections of the soft manipulator.

Table 2: Length variable we input in this simulation

Section number	Length variable vector
i=1	[25 38.5 38.5]
i=2	[38.5 25 38.5]
i=3	[38.5 38.5 25]

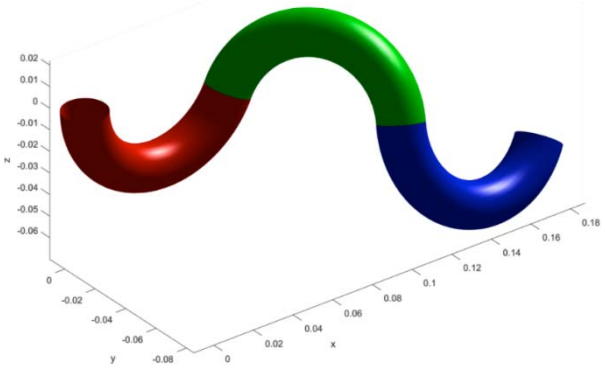

Fig. 7: The simulation result with 9 different length variables

The simulation result is consistent and smooth, and the spatial shape of the three-section manipulator is the same as the assumption we raised. Then, we discuss the situation with a singularity by equalizing the three length variables in the last section, given as table 3. The simulation result is shown as follows.

Table 3: Length variable we input in this simulation

Section number	Length variable vector
i=1	[28.5 27 28.5]
i=2	[25 38.5 38.5]
i=3	[38 38 38]

Authorized licensed use limited to: IEEE Customer. Downloaded on December 27,2020 at 02:07:31 UTC from IEEE Xplore. Restrictions apply.

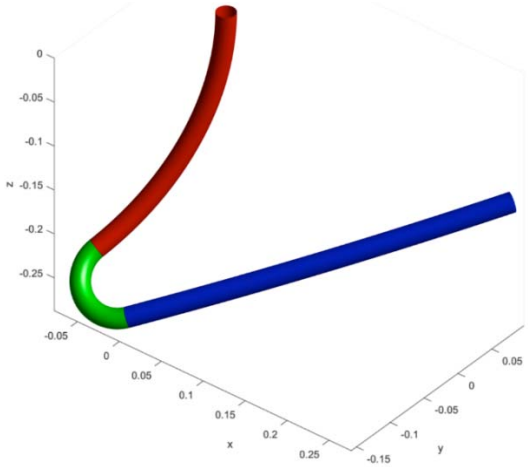

Fig. 8: The simulation result with singularity

It can be seen that the third section is cylindrical to imply that the singularity problem is well solved. So far, the correctness of kinematics model based on curve parameters (include singularity solution) can be preliminarily proved through the above two cases.

4.2 Experiment Validation

This is nowhere near enough to demonstrate the kinematics model only from the theoretical aspect. What we need to do next is to perform experiments by using the prototype we designed. The objective of the following experiments is to imitate common tasks. By means of comparing the simulation result with the prototype in real-time, the effectiveness of the shape detection system of the multi- section soft manipulator is verified.

The experimental process is as follows: We regulate the vent of the proportional valve on the PC to control the pressure of each PMA such that the vertical downward prototype is imposed to bend upward to grasp the foam ball. Meanwhile, the length variables measured by cable encoders are transmitted to the PC as the input of the kinematics model. Through real-time calculation running on MATLAB, the simulation diagram is acquired to show the spatial shape of the soft manipulator. At this time, the prototype and the simulation result are shown relatively as follows:

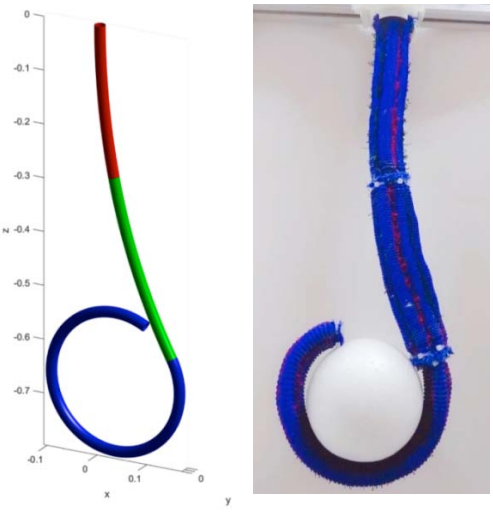

a) Simulation b) Prototype

Fig. 9: The simulation result with 9 different length variables

Secondly, the pressure filled into PMAs is gradually increased to enable the prototype to wrap tightly around the foam sphere. The prototype and simulation result are respectively changed as follows.

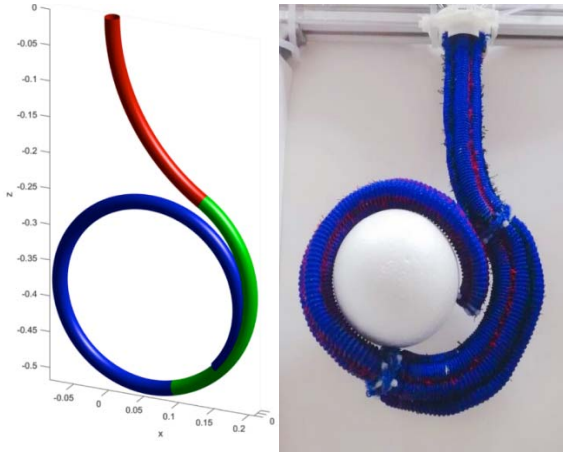

a) Simulation b) Prototype

Fig. 10: The simulation result with 9 different length variables

To sum up, through the contrast of the figure above, it is obvious that the simulation results agree well with the prototype with tiny errors, where the theoretical curvature is larger than the actual one. This is due to the fact that the cable of the cable encoders is not fully attached to the soft manipulator, which causes a little error between the actual length variables and the length variables detected by the cable encoders. Whereas the general shape detection precision requirements for soft manipulator can be fully satisfied.

5 Conclusions

A novel shape detection method for soft manipulator based on curve parameters model is reported in this work. We devise the control system of the soft manipulator for further experimental operation, including the prototype and the sensor network layout mainly. Then, the kinematics model for unit-section and multi-section are developed in turn based on the piecewise constant curvature theory. In addition, the singularity problem is well figured out by the multivariate Taylor expansion. Finally, we verify the shape detection system for the soft manipulator is effective in theory and experiment.

References

[1] A. Chawla, A comparison of constant curvature forward kinematics for multisection continuum manipulators, *in Proceedings of International Conference on Robotic Computing,* 2018: 217-223.

[2] B. Jones, and I. Walker, Kinematics for multisection continuum robots, *Robotics*, 22(1): 43-55, 2006.

[3] D. Rus, Design, fabrication and control of soft robots, *Nature*, 521(7553): 467, 2015.

[4] F. Renda, A 3D steady-state model of a tendon-driven continuum soft manipulator inspired by the octopus arm, Bioinspiration & biomimetics, 7(2): 025006, 2012.

[5] I. Godage, Shape function-based kinematics and dynamics for variable length continuum robotic arms, *in Proceedings of Robotics and Automation*, 2011: 452-457.

[6] I. Godage, Dynamics for biomimetic continuum arms: A modal approach, *in Proceedings of Robotics and Biomimetics*, 2011: 104-109.

[7] I. Godage, Modal kinematics for multisection continuum arms, *Bioinspiration & biomimetics*, 10(3): 035002, 2015.

Authorized licensed use limited to: IEEE Customer. Downloaded on December 27,2020 at 02:07:31 UTC from IEEE Xplore. Restrictions apply.

[8] I. Godage, Novel modal approach for kinematics of multi-section continuum arms, *in Proceedings of Intelligent Robots and Systems*, 2011: 1093-1098.
[9] I. Walker, Kinematics and the implementation of an elephant's trunk manipulator and other continuum style robots, *Journal of robotic systems,* 20(2), 45-63, 2003.
[10] I. Singh, Towards extending forward kinematic models on hyper-redundant manipulator to cooperative bionic arms, *Journal of Physics: Conference Series*, 783(1): 012056, 2017.
[11] J. Santiago, Continuum robots for space applications based on layer-jamming scales with stiffening capability, *in Proceedings of Aerospace Conference*, 2015: 1-13.
[12] M. Sfakiotakis, Octopus-inspired multi-arm robotic swimming, *Bioinspiration & biomimetics*, 10(3): 035005, 2015.
[13] M. Grissom, Design and experimental testing of the octarm soft robot manipulator，*Unmanned Systems Technology VIII*, 6230: 62301F, 2006.
[14] R. Webster III, Design and kinematic modeling of constant curvature continuum robots: A review, *The International Journal of Robotics Research*, 29(13): 1661-1683, 2010.
[15] T. Mahl, A variable curvature continuum kinematics for kinematic control of the bionic handling assistant, *Robotics*, 30(4): 935-949, 2014.
[16] W. Rone, Multi-segment continuum robot shape estimation using passive cable displacement, *in Proceedings of International Symposium on Robotic and Sensors Environments*, 2013: 37-42.
[17] W. Chao, Dynamics control of cable-driven silicone soft manipulator, *Shanghai Jiao Tong University*, 1-z, 2015.
[18] Z. Gong, An Opposite-Bending-and-Extension Soft Robotic Manipulator for Delicate Grasping in Shallow Water, *Front. Robot*. AI 6: 26. doi: 10.3389/frobt, 2019.

Authorized licensed use limited to: IEEE Customer. Downloaded on December 27,2020 at 02:07:31 UTC from IEEE Xplore. Restrictions apply.